Analysis of a Rail Subjected to Mechanical and Thermal Loading

David H. Allen
Gary D. Fry

Center for Railway Research
Texas A&M Transportation Institute
Texas A&M University System

CRR Report No. 2016-01
July 1, 2016

Center for Railway Research

Analysis of a Rail Subjected to Mechanical and Thermal Loading

By

David H. Allen

Gary D. Fry

Abstract

A model is developed herein for predicting the onset of thermally induced lateral buckling in rail structures. As described below, the model may be considered to be an extension of previous efforts spanning most of the twentieth century. Building on both previous analytic and computational solutions, a computational model is developed for the purpose of predicting the thermal buckling temperature as a function of the track and support structure material properties, the track and support system geometries, the applied track loading, and the initial lateral displacement within the track. Particular emphasis is placed on nonlinearity and history dependence of the lateral track resistance to deformation. The resulting model is deployed within a simple Matlab computer program for ease of use by practicing engineers.

Introduction

Rails are known to undergo a variety of failure mechanisms that can cause significant property damage and loss of life (FRA 2015). It is therefore propitious to develop advanced models for the purpose of mitigating such mishaps. Toward this end, a one such model is presented herein.

The literature on this subject is long and deep. Historically, Galileo introduced the problem of a beam in bending in 1637 (Galileo 1637). More than a century later, the first cogent model for beam bending was reported by Euler and Bernoulli (Euler 1744). In the early twentieth century this approach was used to model the structural response of rails (Timoshenko 1915, 1927). Over the most recent half century a rigorous beam formulation of the rail thermal buckling problem has emerged (Kerr 1974, 1978). In addition, methods have been reported for solving the problem numerically (Tvergaard and Needleman 1981, Lim et al 2003).

Model Development

Consider a generic rail mounted on a railway, as shown in Fig. 1. Note that the x coordinate is aligned in the direction of travel, and the y and z coordinate axes are aligned with the vertical and horizontal directions, respectively.

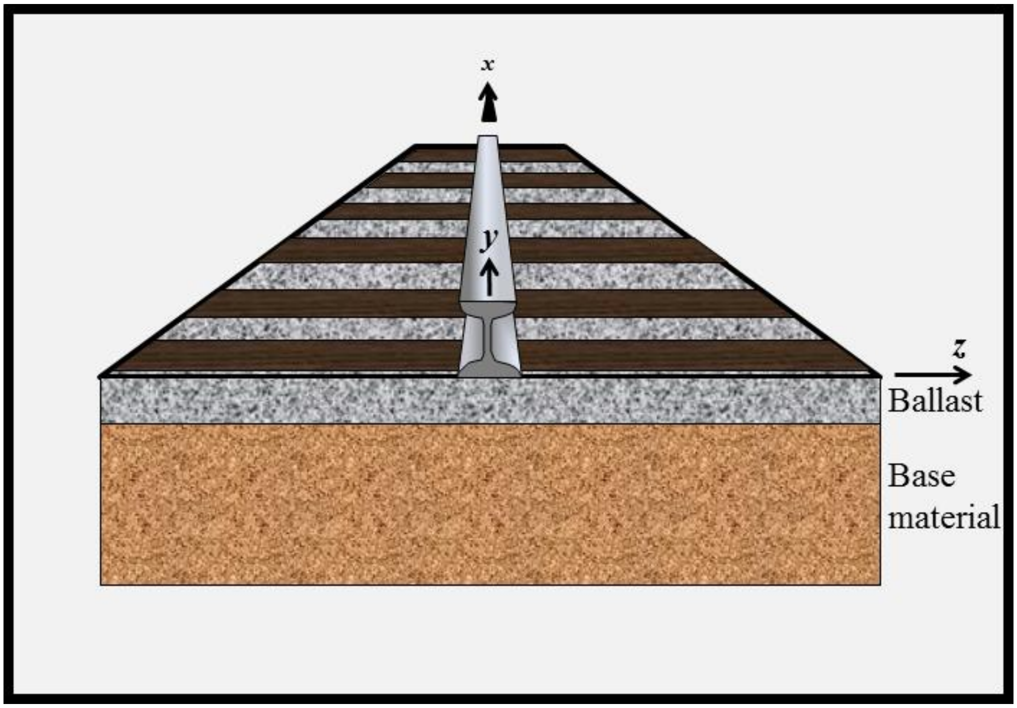

Fig. 1 Generic Rail with Coordinate Axes as Shown

When viewed from the side, a typical rail with mechanical and thermal loading is shown in Fig. 2.

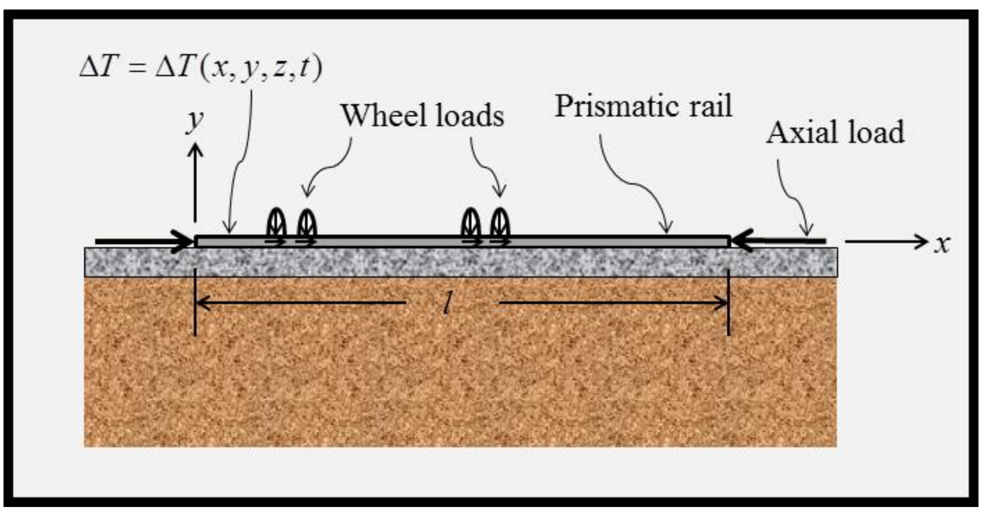

Fig. 2 Typical Rail Loaded Mechanically and Thermally

In order to construct a model of the rail, it is first assumed that it may be modeled as a beam-column, implying that it is long and slender (Allen and Haisler 1985). As shown in Fig. 3, the centroidal axis of the rail may deform in all three coordinate directions, and the components of this displacement are denoted by $u_0(x,t)$, $v_0(x,t)$ and $w_0 = w_0(x,t)$, respectively. Similarly, the components of stress are shown on an arbitrary cross-section of the rail in Fig. 4.

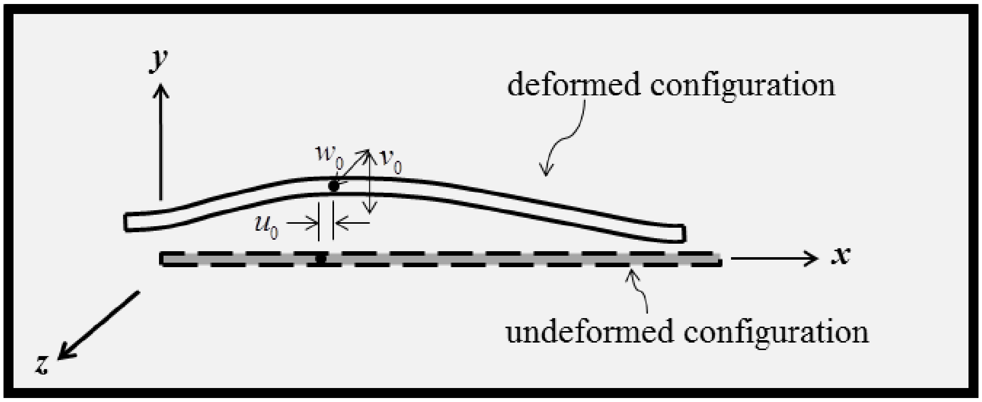

Fig. 3 Depiction of the Rail Showing Displacement Components in the Deformed Configuration

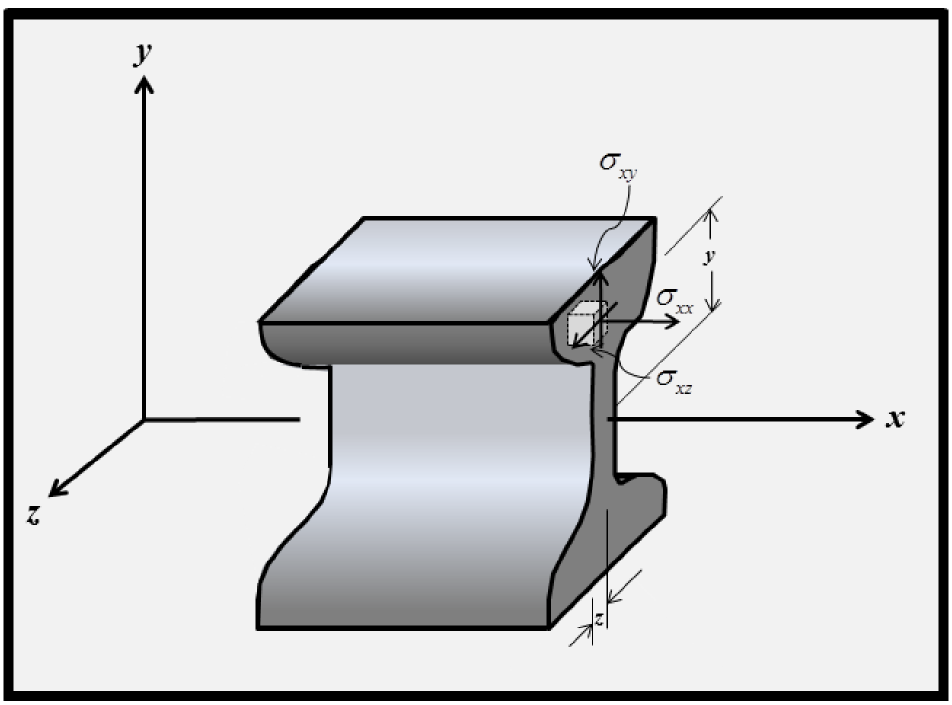

Fig. 4 Components of Stress on an Arbitrary Cross-Section of the Rail

A side view of a free body diagram of a section of the rail is constructed in Fig. 5, wherein the load per unit length applied to the centroidal axis of the rail is composed of components $p_x(x,t)$, $p_y(x,t)$ and $p_z(x,t)$ in the *x, y,* and *z* coordinate directions, respectively. In addition, the normal component of force per unit length applied to the bottom of the rail due to the normal displacement component $v_0(x,t)$ is denoted as $-k_y v_0(x,t)$, where the negative sign is employed so that the base stiffness is non-negative when the resultant is positive due to downward displacement of the rail. Similarly, the axial component of force per unit length applied to the bottom of the rail due to the axial component of displacement $u_0(x,t)$ is denoted as $-k_x u_0(x,t)$, and the out-of-plane component of force per unit length applied to the bottom of the rail due to the z-component of displacement $w_0(x,t)$ is denoted as $-k_z w_0(x,t)$.

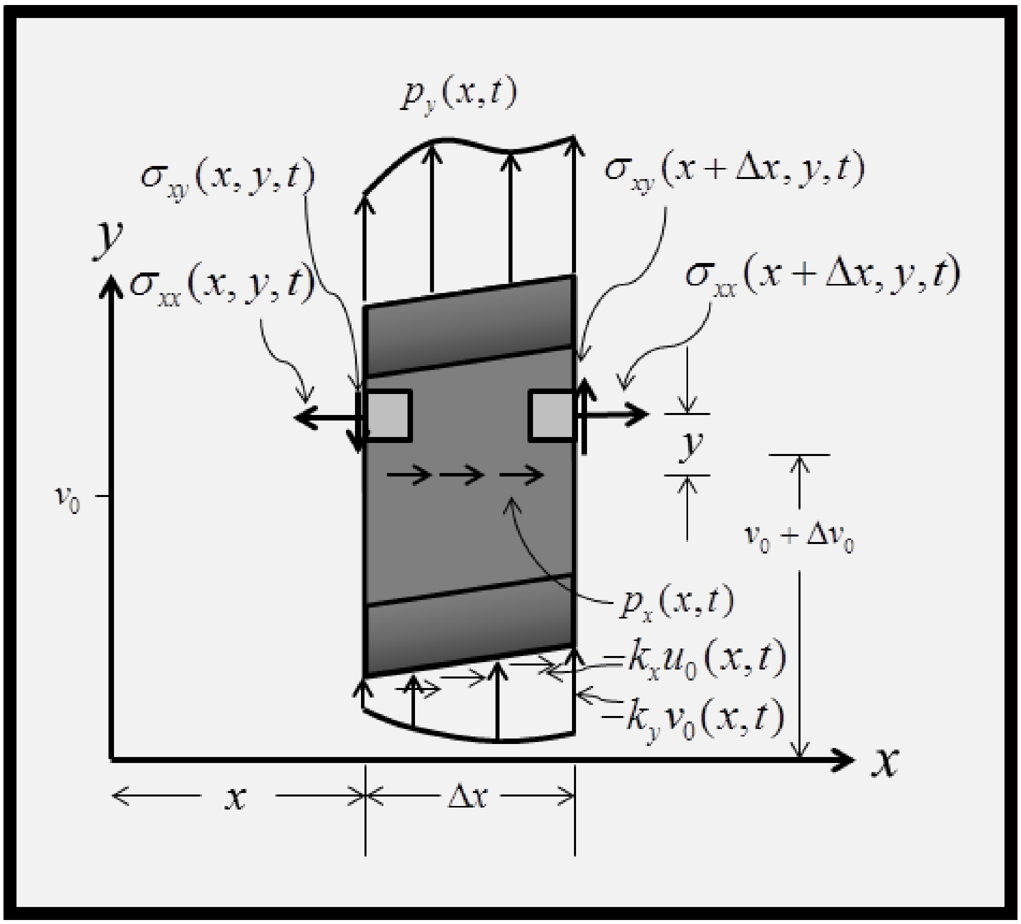

Fig. 5 Free Body Diagram of Cut Rail

Note also that the stress distribution on the two vertical cuts within the rail are denoted generically by the two infinitesimal stress boxes on these faces. Finally, note that the differential element is depicted in the deformed configuration, so that the axial force affects the transverse displacement of the rail. This necessarily causes the response of the rail to be geometrically nonlinear.

Consistent with Euler-Bernoulli beam theory the force and moment resultants are now defined as follows (Allen and Haisler 1985):

$$P = P(x,t) \equiv \int_A \sigma_{xx} dA \tag{1}$$

$$V_y = V_y(x,t) \equiv \int_A \sigma_{xy} dA \tag{2}$$

$$V_z = V_z(x,t) \equiv \int_A \sigma_{xz} dA \tag{3}$$

$$M_y = M_y(x,t) \equiv \int_A \sigma_{xx} z dA \tag{4}$$

$$M_z = M_z(x,t) \equiv -\int_A \sigma_{xx} y dA \tag{5}$$

where A is the cross-sectional area of the rail, and y and z are the vertical and horizontal distance from the centroid, respectively. The above resultants may now be utilized to construct the alternate free body diagram shown in Fig. 6.

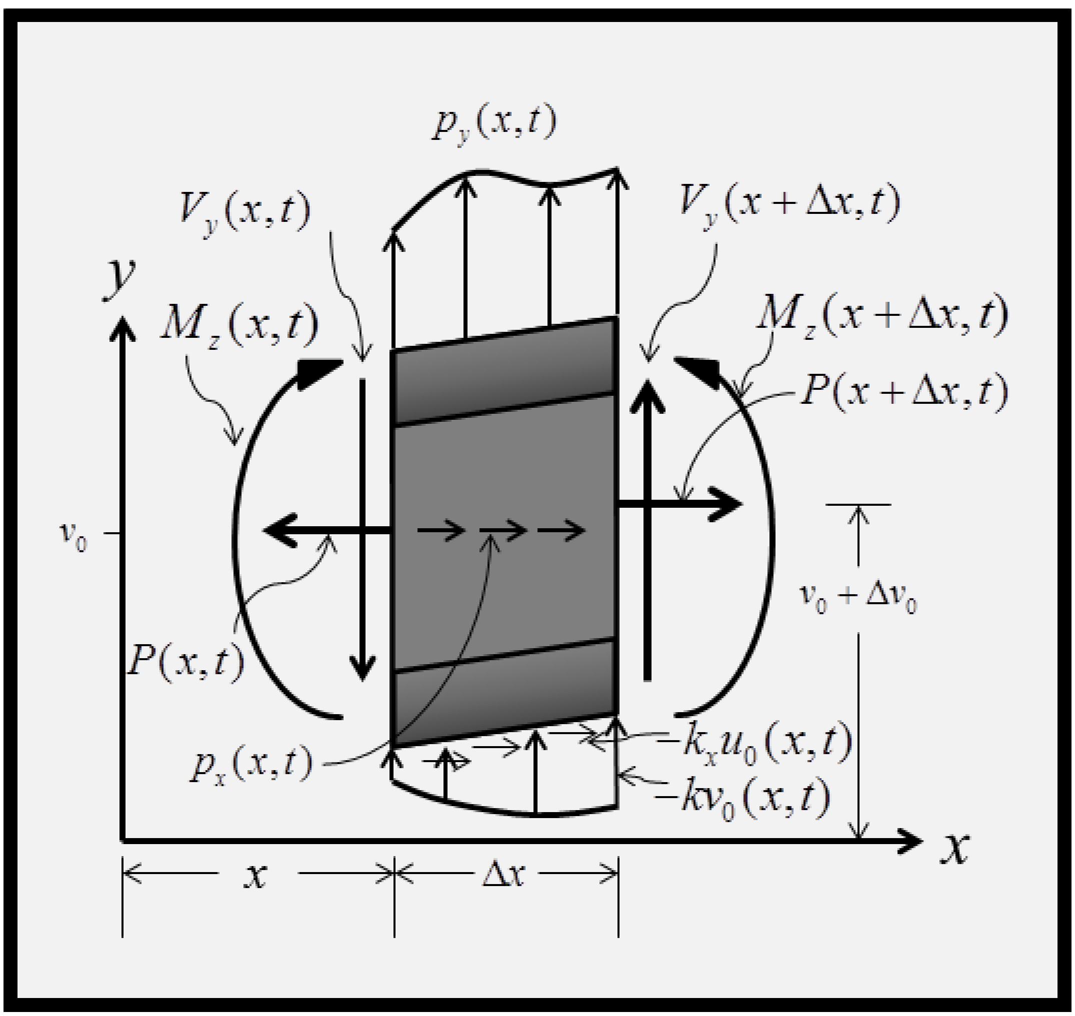

Fig. 6 Resultant Forces and Moments Applied to a Differential element of the Rail

Applying Newton's second law to the forces in the x coordinate direction in Fig. 6 will result in the following (Allen and Haisler 1985):

$$\frac{\partial P}{\partial x} = -p_x + k_x u_0 + \rho A \frac{\partial^2 u_0}{\partial t^2} \tag{6}$$

where, as shown in Fig. 2, *l* is the length of the rail. Similarly, applying Newton's second law to the forces in the y and z coordinate directions will result in the following (Allen and Haisler 1985):

$$\frac{\partial V_y}{\partial x} = k_y v_0 - p_y + \rho A \frac{\partial^2 v_0}{\partial t^2} \tag{7}$$

$$\frac{\partial V_z}{\partial x} = k_z w_0 - p_z + \rho \frac{\partial^2 w_0}{\partial t^2} \tag{8}$$

Also, summing moments about the y- and z-axes and applying Newton's second law will result in the following (Allen and Haisler 1985, Oden and Ripperger 1981):

$$\frac{\partial M_z}{\partial x} = -V_y + P\frac{\partial v_0}{\partial x} + k_x u_0 \frac{h}{2} + \rho I_{zz} \frac{\partial^2 v_0}{\partial t^2} \tag{9}$$

$$\frac{\partial M_y}{\partial x} = V_z + P\frac{\partial w_0}{\partial x} + \rho I_{yy} \frac{\partial^2 w_0}{\partial t^2} \tag{10}$$

where I_{yy} is the second area moment about the y centroidal axis

$$I_{yy} \equiv \int_A z^2 dA \tag{11}$$

and I_{zz} is the second area moment about the z centroidal axis

$$I_{zz} \equiv \int_A y^2 dA \tag{12}$$

Also, *h* is the height of the rail and *w* is the width of the rail.

Equations (6) through (10) can be used, together with boundary and initial conditions, to predict the five unknowns: $P = P(x,t), V_y = V_y(x,t)$, $V_z = V_z(x,t)$, $M_y = M_y(x,t)$ and $M_z = M_z(x,t)$ when the rail is statically determinate. In the general case, however, the problem is much more complex since the displacement components $u_0 = u_0(x,t)$, $v_0 = v_0(x,t)$ and $w_0 = w_0(x,t)$ are also unknowns.

To deal with this issue, the Euler-Bernoulli kinematic assumption is employed, which assumes that planar sections remain planar and normal to the neutral axis of the rail during deformation as shown in Fig. 7 (Allen and Haisler 1985, Allen 2015), thereby resulting in the following assumed form of the axial displacement component:

$$u(x,y,t) = u_0(x,t) - \theta_z(x,t)y + \theta_y(x,t)z \tag{13}$$

where $\theta_y = \theta_y(x,t)$ is the angle of rotation of the vertical plane about the y axis $\theta_z = \theta_z(x,t)$ is the angle of rotation of the vertical plane about the z axis.

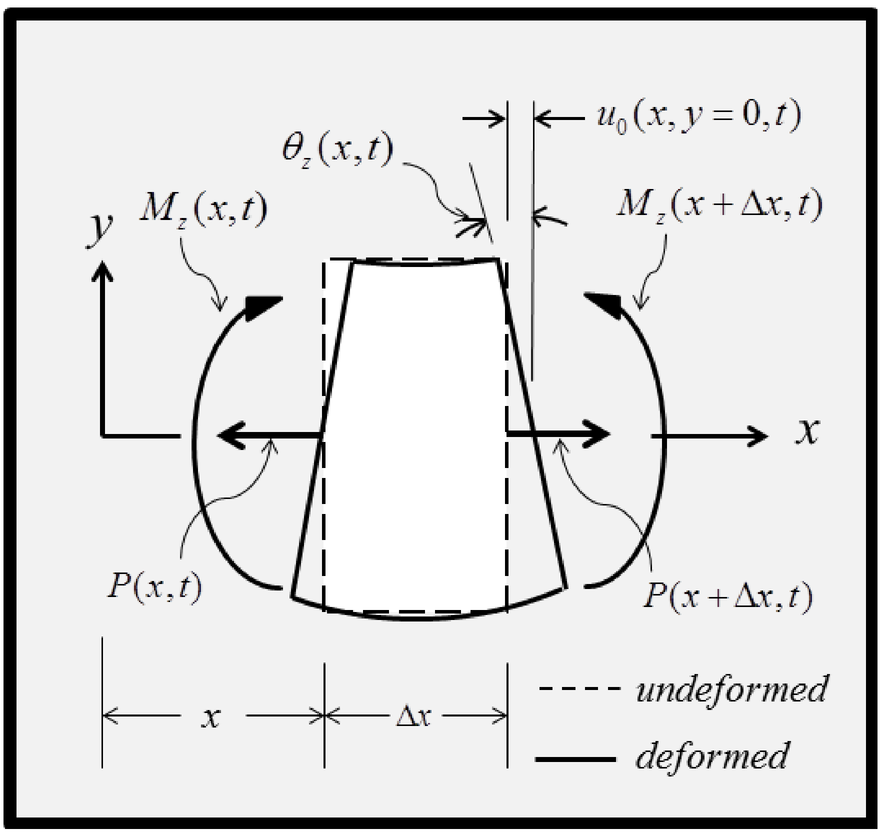

Fig. 7 Kinematics of Deformation of the Euler-Bernoulli Beam

In order to utilize equation (13) to complete the problem description, it is now necessary to introduce the definition of the axial strain, given by:

$$\varepsilon_{xx} \equiv \frac{\partial u}{\partial x} \tag{14}$$

Substituting equation (13) into equation (14) therefore results in the following:

$$\varepsilon_{xx} = \frac{\partial u_0}{\partial x} - y\frac{\partial \theta_z}{\partial x} + z\frac{\partial \theta_y}{\partial x} \tag{15}$$

It is now assumed that

$$\sigma_{yy}, \sigma_{zz} \ll \sigma_{xx} \tag{16}$$

Accordingly, assuming that the rail is linear elastic and isotropic, the constitutive equation for the axial component of the stress, σ_{xx} , may be related to the axial strain component, ε_{xx} , via the following constitutive equation (Allen and Haisler 1985):

$$\sigma_{xx} = E(\varepsilon_{xx} - \alpha\Delta T) \tag{17}$$

where *E* is Young's modulus, α is the coefficient of thermal expansion, and ΔT is the change in temperature (Allen 2013).

Substituting equation (15) into equation (17) and this result into equations (1), (4) and (5) will result in the following:

$$P + P^T = EA\frac{\partial u_0}{\partial x} - EA\bar{y}\frac{\partial \theta_z}{\partial x} + EA\bar{z}\frac{\partial \theta_y}{\partial x} \tag{18}$$

$$M_y + M_y^T = EA\bar{z}\frac{\partial u_0}{\partial x} + EI_{yy}\frac{\partial \theta_y}{\partial x} \tag{19}$$

and

$$M_z - M_z^T = -EA\bar{y}\frac{\partial u_0}{\partial x} + EI_{zz}\frac{\partial \theta_z}{\partial x} \tag{20}$$

where $\bar{y}$ and $\bar{z}$ are the y and z components of the centroid, given by

$$\bar{y} \equiv \frac{1}{A}\int_A ydA \tag{21a}$$

$$\bar{z} \equiv \frac{1}{A}\int_A zdA \tag{21b}$$

and P^T, M_y^T and M_z^T are the thermally induced axial force and bending moment, respectively, given by (Allen and Haisler 1985):

$$P^T \equiv \int_A E\alpha\Delta TdA \tag{22}$$

$$M_y^T \equiv \int_A E\alpha\Delta TzdA \tag{23a}$$

and

$$M_z^T \equiv \int_A E\alpha\Delta TydA \tag{23b}$$

Since the selection of the coordinate axes is arbitrary, we choose to use the centroidal axes, so that $\bar{y} = 0$ and $\bar{z} = 0$, thereby simplifying equations (18) through (20) to the following:

$$P + P^T = EA\frac{\partial u_0}{\partial x} \tag{24}$$

$$M_y + M_y^T = EI_{yy}\frac{\partial \theta_y}{\partial x} \tag{25}$$

and

$$M_z - M_z^T = EI_{zz}\frac{\partial \theta_z}{\partial x} \tag{26}$$

Treating the axial force, *P*, and the bending moments, M_y and M_z, as well as the thermal terms, as if they were known for the time being, equations (24) through (26) can be inverted to the following forms:

$$\frac{\partial u_0}{\partial x} = \frac{(P + P^T)}{EA} \tag{27}$$

$$\frac{\partial \theta_y}{\partial x} = \frac{(M_y + M_y^T)}{EI_{yy}} \tag{28}$$

and

$$\frac{\partial \theta_z}{\partial x} = \frac{(M_z - M_z^T)}{EI_{zz}} \tag{29}$$

Substituting the above three equations into equation (15) results in the following:

$$\varepsilon_{xx} = \frac{(P + P^T)}{EA} - \frac{(M_z - M_z^T)}{EI_{zz}} y + \frac{(M_y + M_y^T)}{EI_{yy}} z \tag{30}$$

Substituting equation (30) into equation (17) results in the following:

$$\sigma_{xx} = \frac{(P + P^T)}{A} - \frac{(M_z - M_z^T)}{I_{zz}} y + \frac{(M_y + M_y^T)}{I_{yy}} z - E\alpha\Delta T \tag{31}$$

Now recall from calculus that (Allen and Haisler 1985)

$$\frac{\partial \theta_y}{\partial x} = \frac{-\dfrac{\partial^2 w_0}{\partial x^2}}{\left[1 + \left(\dfrac{\partial w_0}{\partial x}\right)^2\right]^{3/2}} \approx -\frac{\partial^2 w_0}{\partial x^2} \tag{32}$$

And

$$\frac{\partial \theta_z}{\partial x} = \frac{\dfrac{\partial^2 v_0}{\partial x^2}}{\left[1 + \left(\dfrac{\partial v_0}{\partial x}\right)^2\right]^{3/2}} \approx \frac{\partial^2 v_0}{\partial x^2} \tag{33}$$

Equating (28) and (32) now results in the following:

$$\frac{\partial^2 w_0}{\partial x^2} = -\frac{(M_y + M_y^T)}{EI_{yy}} \tag{34}$$

Similarly, equating (29) and (33) results in the following:

$$\frac{\partial^2 v_0}{\partial x^2} = \frac{(M_z - M_z^T)}{EI_{zz}} \tag{35}$$

It can now be seen that equations (6) through (10), (27), (31), (34) and (35) constitute nine equations in the following nine primary unknowns: $\sigma_{xx}, u_0, v_0, w_0, M_y, M_z, V_y, V_z$ and P. These equations are reproduced for clarity in Table 1. Together with initial and boundary conditions, the model described in Table 1 can be utilized to predict the nine primary variables.

Independent Variables: x,t

Known Inputs:

Loads: $p_x = p_x(x,t), p_y = p_y(x,t), p_z = p_z(x,t), \quad 0 < x < l$

Temperature change: $\Delta T = \Delta T(x,y,z,t) = known$

Geometry: l, h, A, I_{yy}, I_{zz}

Material Properties: $\rho, \alpha, E, k_x, k_y, k_z$

Unknowns: $u_0, v_0, w_0, \sigma_{xx}, P, V_y, V_z, M_y, M_z$ **= 9 unknowns**

Field Equations:

Equation	No. of Equations
$\frac{\partial P}{\partial x} = -p_x + k_x u_0 + \rho A \frac{\partial^2 u_0}{\partial t^2}$	1
$\frac{\partial V_y}{\partial x} = k v_0 - p_y + \rho A \frac{\partial^2 v_0}{\partial t^2}$	1
$\frac{\partial V_z}{\partial x} = k_z w_0 - p_z + \rho \frac{\partial^2 w_0}{\partial t^2}$	1
$\frac{\partial M_y}{\partial x} = V_z + P \frac{\partial w_0}{\partial x} + \rho I_{yy} \frac{\partial^2 w_0}{\partial t^2}$	1
$\frac{\partial M_z}{\partial x} = -V_y + P \frac{\partial v_0}{\partial x} + k_x u_0 \frac{h}{2} + \rho I_{zz} \frac{\partial^2 v_0}{\partial t^2}$	1
$\sigma_{xx} = \frac{(P + P^T)}{A} - \frac{(M_z - M_z^T)}{I_{zz}} y + \frac{(M_y + M_y^T)}{I_{yy}} z - E\alpha\Delta T$	1
$\frac{\partial u_0}{\partial x} = \frac{(P + P^T)}{EA}$	1
$\frac{\partial^2 w_0}{\partial x^2} = -\frac{(M_y + M_y^T)}{EI_{yy}}$	1
$\frac{\partial^2 v_0}{\partial x^2} = \frac{(M_z - M_z^T)}{EI_{zz}}$	1
Total	**9**

Table 1 Model for Predicting the Rail Response

The procedure utilized to solve this problem will depend on the initial and boundary conditions, as well as certain simplifying approximations deployed for the purpose of solving the problem. The case of thermal buckling will be considered in the following section.

Thermal Buckling

A common cause of rail misalignment is thermal buckling, as shown in Fig. 8. Note from the photograph that buckling normally occurs laterally. This is due to the fact that the moment of inertia of the rail about the vertical axis is significantly lower than that about the horizontal axis.

Fig. 8 Photograph Showing Thermally Induced Buckling of a Railway

Thermal buckling can be rather complicated depending on the temperature distribution within the rails and the structural configuration of the underlying railway base. However, a fairly simple first approximation can be made, and it will be described in this section. The following assumptions are made to obtain this simplified solution:

1) the only axial load occurs due to temperature;
2) the temperature is spatially homogeneous but increases linearly in time;
3) dynamic effects can be neglected;
4) prior to buckling the rail is constrained against motion in the x coordinate direction;
5) there is no distributed load applied to the rail in the z coordinate direction; and
6) there is no bending about the z axis.

Under the above assumptions the problem simplifies to that shown in Table 2.

Independent Variables: x,t

Known Inputs:

Loads: $p_z = 0$

Temperature change: ΔT

Geometry: l, h, A, I_{yy}, I_{zz}

Material Properties: ρ, α, E, k_z

Unknowns: $w_0, \sigma_{xx}, P, V_z, M_y$ **= 5 unknowns**

Field Equations:

	Equation	No. of Equations
(T2.1)	$\dfrac{\partial P}{\partial x} = 0$	1
(T2.2)	$\dfrac{\partial V_z}{\partial x} = k_z w_0 - p_z$	1
(T2.3)	$\dfrac{\partial M_y}{\partial x} = V_z + P\dfrac{\partial w_0}{\partial x}$	1
(T2.4)	$\sigma_{xx} = \dfrac{(P + P^T)}{A} + \dfrac{(M_y + M_y^T)}{I_{yy}} z - E\alpha\Delta T$	1
(T2.5)	$\dfrac{\partial^2 w_0}{\partial x^2} = -\dfrac{(M_y + M_y^T)}{EI_{yy}}$	1
	Total	**5**

Table 2 Simplified Model for Predicting Thermally Induced Rail Buckling

It can be seen from equations (22) and (27), as well as assumption 4) that

$$P(t) = -P^T(t) = -EA\alpha\Delta T \tag{36}$$

$$M_y^T = 0 \tag{37}$$

thereby providing one of the unknowns. The physically important unknowns are $w_0(x,t)$ and $\sigma_{xx}(x,t)$. In order to predict these unknowns with the model it is necessary to apply initial and boundary conditions. These are assumed to be as follows:

I.C.: $w_0(x, t=0) = 0 \qquad \forall x \in 0, l$ (38a)

B.C.: $w_0(x=0, t) = 0,\ w_0(x = l_B, t) = 0$ (38b)

B.C.: $\dfrac{\partial w_0}{\partial x}(x=0, \mathrm{t}) = 0,\ \dfrac{\partial w_0}{\partial x}(x = l_B, t) = 0$ (38c)

where l_B is the length of the buckle in the rail.

Because the boundary conditions are all of displacement type it is possible to reduce the governing equations to a single primary equation in terms of the transverse displacement component, $w_0(x,t)$. To do this, first rearrange equation (T2.3) and substitute this result into equation (T2.2) to obtain the following:

$$\frac{\partial}{\partial x}\left(\frac{\partial M_y}{\partial x} - P^T \frac{\partial w_0}{\partial x}\right) = k_z w_0 - p_z \tag{39}$$

Next rearrange equation (T2.5) and substitute into the above, thereby resulting in the following equation:

$$EI_{yy}\frac{\partial^4 w_0}{\partial x^4} + P^T \frac{\partial^2 w_0}{\partial x^2} + k_z w_0 = p_z \tag{40}$$

Note that the above equation reduces to the equation for simple beams if $P^T = k_z = 0$.

The exact solution to the homogeneous part of equation (40) is given by the following:

$$w_0^H(x) = A_1 \sin\lambda x + A_2 \cos\lambda x \tag{41}$$

where

$$\lambda = \sqrt{\frac{P^T}{EI_{yy}}} \tag{42}$$

Substituting equation (41) into the homogeneous part of equation (40) results in the following:

Substituting (38b) and (38c) into equation (41) results in the following:

$$w_0(x) = A_0\left[1 - \cos\left(\frac{2\pi x}{l}\right)\right] \tag{43}$$

In order to determine the unknown coefficient A_0 it is necessary to substitute equation (43) into equation (40), thereby resulting in the following constraint on the exact solution:

$$A_0 = \frac{p_z}{k_z} \tag{44}$$

Since equation (43) results in a homogeneous governing equation, it follows that:

$$P_{cr}^T = \frac{k_z l^2}{4\pi^2} + \frac{4\pi^2 EI_{yy}}{l^2} \tag{45}$$

where P_{cr}^T is the critical thermally induced axial load that will cause rail buckling. Also, the first term on the right hand side shows the effect of lateral friction against buckling, and the second term is the classical column buckling term.

To obtain the critical temperature at which rail buckling is predicted, substitute equation (22) into equation (45) and solve for the critical temperature change, ΔT_{cr}:

$$\Delta T_{cr} = \frac{1}{E\alpha A}\left(\frac{k_z l^2}{4\pi^2} + \frac{4\pi^2 EI_{yy}}{l^2}\right) \tag{46}$$

Note that the critical temperature is independent of the laterally applied load per unit length, p_z. As in classical buckling theory, the critical buckling temperature depends only on the rail geometry and material properties. However, in this case it also depends on one additional material property, the coefficient of friction between the rail and ballast in the z coordinate direction, k_z. For purposes of demonstration, the above equation is analyzed using the material properties shown in Table 1.

Property	Value	Units
E	$2.06\text{x}10^5$	MPa
α	$1.05\text{x}10^{-5}$	1/°C
A	$1.45\text{x}10^{-2}$	m^2
I_{yy}	$8.99\text{x}10^{-6}$	m^4

Table 1 Properties Utilized to Perform Analyses Shown in Figs. 9 and 10 (Kerr 1978, Tvergaard and Needleman 1981)

As shown in Fig. 9, the predicted critical temperature is significantly affected by the length of the rail buckle. Note that in geographic areas wherein in temperature changes in excess of 60°C are possible the track friction coefficient is essential to the resistance to buckling. In fact, it is apparent that buckle lengths of 6 m or more in length are possible when lateral friction is negligible. Furthermore, the critical temperature for buckling actually *increases* with increasing lateral friction. For example for track friction coefficients in excess of 1.0 MPA, temperature changes of at least 80°C are necessary to produce track buckling (of approximately 7 m in length).

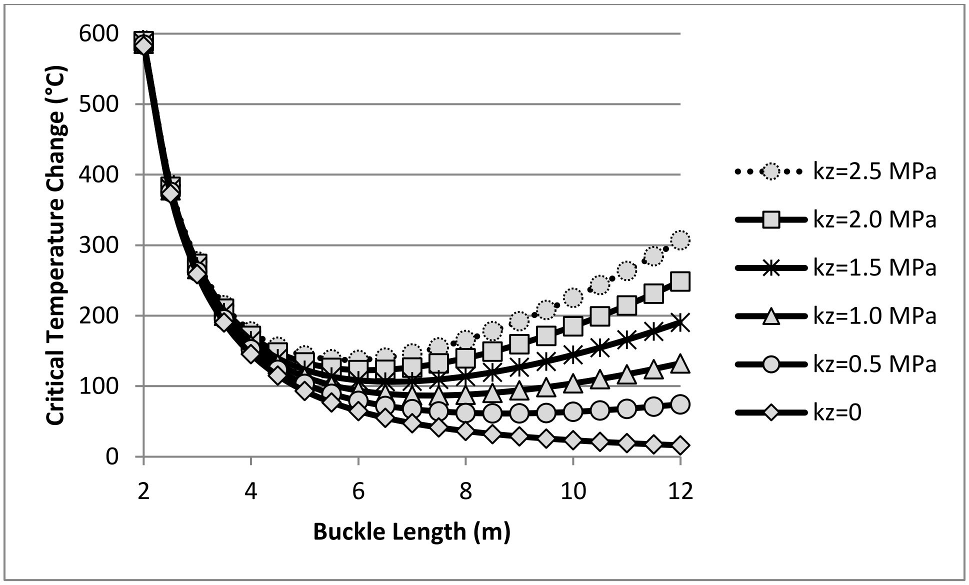

Fig. 9 Predicted Critical Temperature Change for Rail Buckling as a Function of Buckle Length for Three Different Friction Coefficients

Perhaps more importantly, the critical temperature is also strongly affected by the lateral coefficient of friction, k_z, as shown in Fig. 10. Whereas longer buckle lengths are possible at lower values of temperature change when track friction is negligible, this trend reverses when there is significant track friction. Thus, providing lateral friction between the rail and ballast may significantly reduce rail buckling due to temperature change.

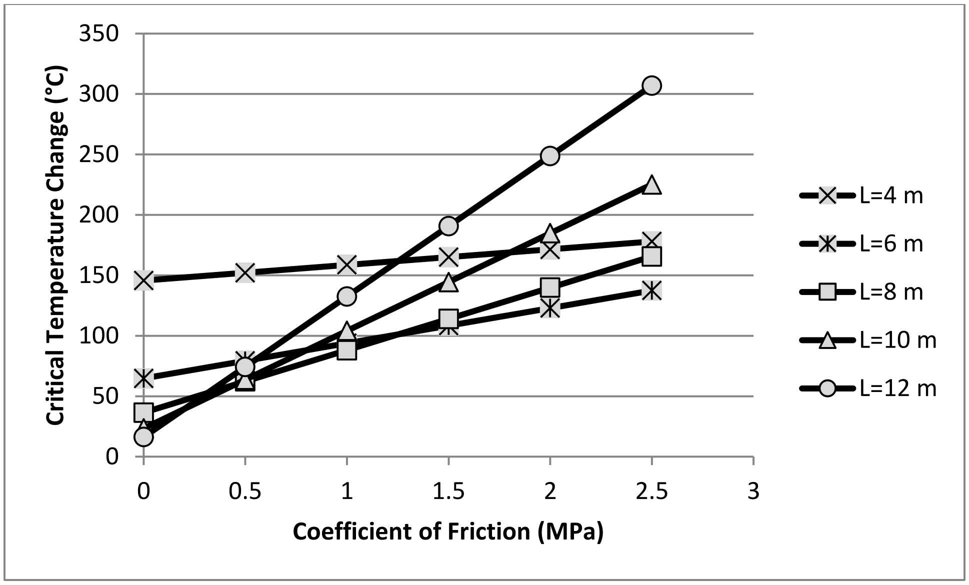

Fig. 10 Predicted Critical Temperature Change for Rail buckling as a Function of Friction Coefficient for Three Different Buckle Lengths

Conclusion

These results suggest the following two ways of mitigating thermal buckling of rails:

1) provide lateral structural support to rails at intervals predetermined by local temperature extremes as a means of obviating thermally induced buckling; and/or
2) imbedding friction enhancement devices within the ballast coarse as a means of increasing lateral friction within the railway.

Unfortunately, it is noteworthy that while the model developed herein suggests some possibilities for mitigating thermally induced rail buckling, it does not result in an situ means of anticipating rail buckling based on the observation of rail deformations due to the fact that indeed no deformations are predicted by the model prior to buckling. Rather, the model developed here in suggests that a more appropriate variable to be monitored as a predictor of rail buckling is the rail temperature.

Acknowledgment

References

D Allen and W Haisler (1985) Introduction to aerospace structural analysis, Wiley

D Allen (2013) Introduction to the mechanics of deformable solids: bars and beams, Springer

L Euler (1744) Method inveniendi lineas curvas, Opera Omni, St. Petersburg, Russia

G Galileo (1637) Dialogues concerning two new sciences, Dover

A Kerr (1974) The stress and stability analyses of railroad tracks, J Appl Mech, 41:841-848

A Kerr (1978) Analysis of thermal track buckling in the lateral plane, Acta Mechanica, 30:17-50

N Lim, N Park and Y Kang (2003) Stability of continuous welded track, Computers & Structures, 81:2219-2236

J Oden and E Ripperger (1981) Mechanics of elastic structures, Second Edition, McGraw-Hill

Railroad Accident Statistics (2015) Federal Railroad Administration, downloaded at:http://safetydata.fra.dot.gov/officeofsafety/publicsite/Query/TrainAccidentsFYCYWithRates.aspx

S Timoshenko (1915) Strength of rails, Transactions of the Institute of Ways and Communications, St. Petersburg, Russia

S Timoshenko (1927) Method of analysis of statical and dynamical stresses in rail, Proc. Second International Congress for Applied Mechanics, Zurich

V Tvergaard and A Needleman (1981) On localized thermal track buckling, Int J Mech Sci, 23:577-587